

Evaluation of the effect of 3D-bioprinted gingival fibroblast-encapsulated ADM scaffolds on keratinized gingival augmentation

Peng Liu^{1,2,3} | Qing Li^{1,2,3} | Qiaolin Yang^{3,4} | Shihan Zhang⁵ | Ke Yi¹ |
Guifeng Zhang⁶ | Zhihui Tang¹

¹Second Clinical Division, Peking University School and Hospital of Stomatology, Beijing, 100101, P. R. China

²Center of Digital Dentistry, Peking University School and Hospital of Stomatology, Beijing, 100081, P. R. China

³National Center of Stomatology and National Clinical Research Center for Oral Diseases and National Engineering Research Center of Oral Biomaterials and Digital Medical Devices, Beijing, 100081, P. R. China

⁴Department of Orthodontics, Peking University School and Hospital of Stomatology, Beijing, 100081, P. R. China

⁵Department of Geriatric Dentistry, Peking University School and Hospital of Stomatology, Beijing, 100081, P. R. China

⁶State Key Laboratories of Biochemical Engineering, Institute of Process Engineering, Beijing, 100190, P. R. China

Correspondence

Zhihui Tang, Second Clinical Division, Peking University School and Hospital of Stomatology, 66 Anli Avenue, Chaoyang District, Beijing 100101, P. R. China.
Email: zhihui_tang@bjmu.edu.cn

Funding information

National Key Research and Development Program of China, Grant/Award Number: 2017YFA0701302; Foundation PKUSS20200113

Abstract

Background and Objectives: The keratinized gingiva plays an important role in maintaining healthy periodontal and peri-implant tissue. Acellular dermal matrix (ADM), as a substitute biomaterial, has a porous structure and good biocompatibility. 3D-bioprinting has the potential for tissue engineering because it enables precise loading of cells layer-by-layer. Herein, we bioprinted ADM scaffold encapsulating gingival fibroblasts (GFs) and evaluated its efficacy in keratinized gingiva augmentation in vivo to assess its potential for clinical periodontal tissue regeneration.

Methods: GFs were extracted from the gingiva of beagles and transfected with a green fluorescent protein (GFP). The ADM scaffold (ADM cell-free group) was constructed using ADM, gelatin, and sodium alginate mixed at an appropriate ratio via 3D-bioprinting. The ADM cell scaffold (ADM cell group) was established by adding extra GFs in the same manner. Six beagles were divided into blank control, ADM cell-free, and ADM cell groups; and implant surgery was performed. The keratinized gingiva was clinically and histologically evaluated at baseline and after 2 months.

Results: GFs transfected with GFPs expressed green fluorescence and were present in new tissue in the ADM cell group and not observed in the ADM cell-free group. At 2 months after surgery, the keratinized gingival augmentation in the ADM cell group was significantly more than that in the ADM cell-free group. Attached gingival augmentation was also observed more in the ADM cell group than that in the ADM cell-free group. Histological staining showed that the tissue in the ADM cell group displayed a more integrated structure and higher expression of COL I, COL III, and VEGF-A than those in the ADM cell-free group.

Conclusion: 3D-bioprinted GF-encapsulated ADM scaffolds increased the amount of keratinized gingiva in vivo, suggesting that 3D-bioprinting has great potential for oral soft tissue regeneration.

KEYWORDS

3D-bioprinting, acellular dermal matrix, keratinized gingiva augmentation, gingival fibroblasts

Peng Liu and Qing Li authors contributed equally to this work.

© 2023 John Wiley & Sons A/S. Published by John Wiley & Sons Ltd.

1 | INTRODUCTION

Keratinized gingiva is important for maintaining healthy teeth and implants.¹⁻⁴ A variety of surgical approaches have been developed to reconstruct keratinized gingiva, among which the autogenous tissue graft is the gold standard in terms of stability and predictability.⁵ However, autogenous tissue grafts have limitations for long-term clinical application, such as limited supply of donor tissue, postoperative pain, increased operation time, and potentially unsatisfactory aesthetic outcomes.⁶⁻⁸ For these reasons, alternate materials and new technologies are needed for keratinized gingival augmentation.

Collagen-based materials have superior biological properties and are used extensively in craniofacial clinical practice.^{9,10} Acellular dermal matrix (ADM), a cell-free scaffold mainly composed of collagen, is widely used for periodontal tissue regeneration and root coverage of teeth and implants.^{11,12} ADM minimizes patient discomfort and reduces the risk of complications at the donor site. Also, ADM yields similar esthetic results compared with autogenous graft. However, ADM was not convenient to conduct the personalized regenerative repair during the operations, and is difficult for regeneration of critical amount of keratinized tissue, such as tumor and trauma^{13,14} due to lacking the autologous tissue cells. To solve the problems of customization, an ADM bioink was produced and the biocompatibility was proved.¹⁵ This lays a foundation to achieve the 3D-bioprinted cell encapsulated ADM scaffold.

Three-dimensional (3D) cell printing technology based on computer-aided design techniques to stack cell-laden materials layer-by-layer into 3D structures enables individualized fabrication. It enables the delivery of cell-laden materials with high spatial precision to approximate the sophisticated and orderly structures of natural tissues,¹⁶⁻¹⁸ enjoying great potential for tissue regeneration and repair, such as vessels, skin, bone, heart, and nerves.¹⁹⁻²³ The precise distribution of cells and porous structure in the 3D scaffold promote cell adhesion and proliferation. 3D cell printing can repair large-scale tissue defects following large-scale *in vitro* expansion of cell-binding materials. In addition, *in situ* printing of regenerated tissue would reduce surgery duration, pain, and discomfort. In oral regenerative medicine, 3D cell printing is viewed as a novel approach for precise treatment and customized tissue defect repair.²⁴⁻²⁶

In previous studies, we used GFs as seed cells and ADM as the matrix for 3D-bioprinting. A two-layer structure scaffold (dense outer layer and loose inner layer) was prepared, and its performance was tested *in vitro*.¹⁵ In this study, we evaluated the ability of the scaffold to increase the quality and quantity of keratinized gingiva *in vivo*, to assess its clinical potential for periodontal tissue regeneration.

2 | MATERIALS AND METHODS

2.1 | Experimental animals

Six healthy beagles (mean age, 12–15 months; mean body weight, 8–10 kg) were used in this study. The animals were raised individually

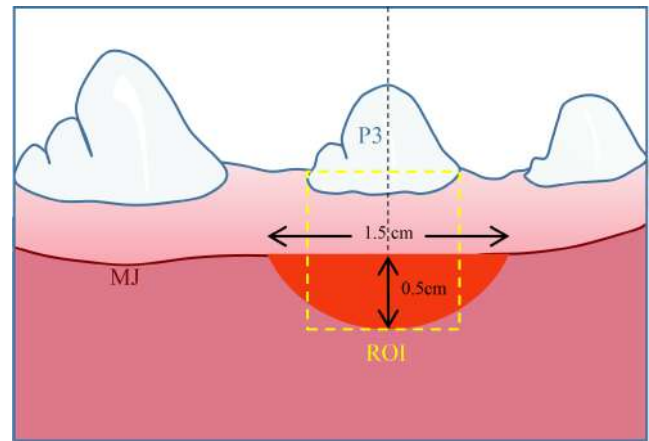


FIGURE 1 Schematic diagram of the defect. The distance from the two ends of the incision to the long axis of the teeth passing through the P3 tip was equal. The vertical distance between the lower edge midpoint and the upper edge midpoint of the defect was 0.5 cm. The horizontal position of the ROI was determined at the area between the mesial gingiva margin and distal gingiva margin of P3, and its vertical range was from the gingival margin to the bottom edge of defect. P3, the third premolar; MJ, mucogingival junction; ROI, region of interest.

under standard laboratory conditions and were in good physical condition with a healthy periodontal status. The study was approved by the Ethics Committee of Peking University School of Stomatology (LA2018006).

2.2 | Clinical measurements

The beagles were stabilized by inhalation anesthesia, and the plaque index (PLI), bleeding on probing (BOP), probing depth (PD), and width of keratinized gingiva (KGW) in the region of interest (ROI) were measured at baseline and 2 months after the operation. The horizontal position of the ROI was determined at the area between the mesial gingiva margin and distal gingiva margin of the third premolar (P3), and its vertical range was from the gingival margin to the bottom edge of the defect (Figure 1).

A Williams periodontal probe was used to measure the PD and KGW of P3 of the bilateral mandible. The position of the mucogingival junction was determined by the Roll test, and Schiller's iodine solution was used for verification.^{27,28} The KGW represents the distance from the free gingival margin to the mucogingival junction. The KGW of three sites (mesiobuccal, mid-buccal, and distobuccal) was measured along the tooth longitudinal axis with reference to the mesial gingiva margin, midpoint of gingiva margin (corresponding to the midpoint of the tooth cusp), and distal gingiva margin of the tooth. The width of the attached gingiva (AGW) is the difference between the KGW and PD.

All measurements were performed independently by two experienced periodontists. A consistency check was conducted before the measurements ($\kappa=0.85$). To reduce deviation, subsequent surgical operations were performed by a third professional periodontist.

2.3 | Extraction and cultivation of GFs

A 2-mm³ biopsy (including epithelial and connective tissue) of gingiva from the hard palate was collected for GF extraction. Gingival tissue samples were immediately placed in sterile phosphate-buffered saline (PBS) (Gibco-Invitrogen, Life Technologies) containing 1% antibiotics (penicillin and streptomycin; Gibco-Invitrogen). The tissue was gently shredded into <1mm³ pieces and digested with collagenase and trypsin (Gibco) for 60 min. Next, the tissue pieces were seeded into a culture bottle and incubated in growth medium (GM), composed of Dulbecco's modified Eagle's medium enriched with 10% fetal bovine serum (Gibco) and 1% penicillin and streptomycin, in the presence of 5% CO₂ at 37°C.^{29,30} The culture medium was changed every 2 days. When the primary cells (P0) reached 80%–90% confluence, the trypsin digestion solution was added at 37°C for 3 min; subsequently, the medium was added to terminate digestion. First-generation (P1) cells were subcultured at a ratio of 1:2. Passage-3–4 GFs were used for subsequent experiments.

2.4 | Preparation of GFs stably expressing green fluorescent protein

To label transplanted GFs, cells were transfected with green fluorescent protein (GFP). Recombinant lentivirus containing GFP was purchased from GenePharma Co. GFs were inoculated in a 10-cm culture dish at a density of 1×10^5 . When the cell density reached 70%, 100 µL of lentiviral reagent (MOI=50) and a final concentration of 5 µg/mL polybrene were added to the culture medium. Lentivirus-containing medium was replaced with a fresh medium after 24 h, and GFP expression was observed under an inverted fluorescence microscope after 2–3 days. Medium containing 10 µg/mL puromycin was used to select cells expressing GFP, which were passaged and expanded independently for use in subsequent experiments.

2.5 | 3D-bioprinted scaffold fabrication

ADM was extracted from porcine skin as described previously. Bioink was prepared with ADM, gelatin, and sodium alginate at a ratio of 6: 2: 2% (wt%). GFs expressing GFP were digested with trypsin, mixed evenly with bioink, and printed using a 3D cell printer (Medprin). The printed scaffold consisted of two alternately printed layers (dense and porous layers). The dense layers have small pores to ensure the strength of the scaffold, and the porous layers have larger pores to facilitate culture of cells and blood vessels. Finally, cell-containing (ADM cell) and cell-free (ADM cell-free) scaffolds were printed and transferred to a fresh culture medium. The cells in the scaffold were observed and photographed using a confocal fluorescent microscope (Carl Zeiss).

2.6 | Animal surgery

A total of 12 sites (two sites in each of six animals) were treated. The 12 sites were randomly divided into blank control, ADM cell-free, and ADM cell groups. The surgery was performed on P3 of the mandible on both sides.

The animal experiments were conducted in accordance with the ethical guidelines of the Institutional Animal Care and Use Committee of Peking University. Implantation surgery was performed on six healthy male Beagles.²⁸ The Beagles fasted with water for 8–12 h before surgery. After inducing anesthesia with 3% pentobarbital sodium (1 mL/kg, intravenous), the animals were placed in the supine position and intubated. Next, 75% alcohol was used to disinfect the skin around the mouth, and 0.12% chlorhexidine for oral rinsing.

- a. A 1.5-cm-long horizontal incision was made along the buccal mucogingival junction of P3. The distance from the two ends of the incision to the long axis of the tooth passing through the P3 tip was equal as shown in Figure 1.
- b. A partial-thickness flap was turned toward the root, repositioned apically, and then secured with periosteal suture (Coated polyglactin 910 suture, 6-0, ETHICON, Inc.). The vertical distance between the lower edge midpoint and the upper edge midpoint of the defect was 0.5 cm.
- c. In the ADM cell group, the 3D-bioprinting complex was implanted (with the dense layer to the outside and porous layer to the exposed tissue surface) into the defect. In the ADM cell-free group, the ADM scaffold without cells was placed in the same position. In the blank control group, no material was placed. All materials were fixed using crossed mattress suture with 6-0 absorbable Coated polyglactin 910 suture (ETHICON, Inc.) in three groups and tied loosely.
- d. Sterile aluminum foil was placed in the surgical area to cover the wound and fixed. Then a periodontal plug was placed on the outer layer. All treatments were performed on each side of the mandible bilaterally, and the treatments were randomly assigned to the defects for minimizing the possible effects of different sites for the outcomes. Besides, to ensure the standardization and consistency of the defect, the periodontal surgeries were performed by the same experienced periodontal surgeon. The surgeries were performed aseptically, and the suffering of the animals was minimized.
- e. Liquid food was provided for 3 days after surgery, and antibiotics were administered intravenously for 1 week. The periodontal plug preparation and aluminum foil were removed as appropriate 2 weeks after surgery. A toothbrush and 0.12% chlorhexidine were used three times per week for plaque control.

2.7 | Histologic evaluation

Part of the gingival tissue in the surgery area was obtained and fixed with 4% paraformaldehyde for 24 h at 4°C. The tissue was

dehydrated using gradient concentrations of sucrose and embedded in OCT. The OCT-embedded tissue was frozen and sectioned for immunofluorescence. The fluorescence of newly formed tissue was visualized using a confocal laser scanning microscope (Carl Zeiss).

2.7.1 | Hematoxylin and eosin (H&E), Masson and Sirius Red staining

Mandibles were fixed in 4% paraformaldehyde for 48 h and decalcified in 10% ethylenediaminetetraacetic acid (EDTA) for 6 months. The specimens were dehydrated in a graded series of ethanol, cleared with xylene, embedded in paraffin, and sectioned at 5- μ m thickness. The sections were stained with H&E, Masson's trichrome stain, and Sirius Red for histological observation according to the manufacturer's protocol. For H&E staining, the slides were stained with Hematoxylin solution (Solarbio) for 5 min and Eosin dye (Solarbio) for 2 min. For Masson's trichrome staining, the slides were soaked in 2.5% potassium dichromate mordant overnight and rinsed with running water. Then the slides were successively immersed in Weigert iron hematoxylin dye solution for 1 min, differentiated with 1% hydrochloric acid alcohol for 1 s, and soaked in ponceau acid fuchsin for 6 min. Finally, the slides were immersed in 1% phosphomolybdic acid solution for 1 min and 2.5% aniline blue solution for 30 s according to the manufacturer's protocol (Servicebio). Collagen is blue-stained under optical microscope. For Sirius Red staining, the sections were incubated with Sirius Red solution (Servicebio) for 8 min and rinsed with running water. The slides were dehydrated with anhydrous ethanol, transparent with xylene, and sealed with neutral gum. Collagen and non-collagen components were red- and orange-stained under optical microscope, respectively.

2.7.2 | Immunohistochemistry

Epitope retrieval was accomplished by heating at 95°C in citrate solution (Solarbio) for 15 min. Sections were blocked in 5% goat serum albumin (ZSGB-Bio), and incubated with primary antibodies against type I collagen (COL I) (GeneTex), type III collagen (COL III) (Proteintech), and vascular endothelial-derived growth factor-A (VEGF-A) (Abcam) overnight at 4°C, followed by the appropriate secondary antibodies (ZSGB-Bio) for 1 h. Signals were visualized using a DAB Detection Kit (ZSGB-Bio) and sections were counterstained with hematoxylin. Images were captured using a light microscope (Olympus) and quantitation was carried out using ImageJ software (NIH).

2.8 | Statistical analysis

Statistical analysis was performed using SPSS software (ver. 22.0; IBM Corp.). Two-tailed unpaired Student's *t*-test was used for

the comparison of two groups, and one-way analysis of variance (ANOVA) for the comparison of more than two groups. Results are presented as mean \pm standard deviation. A *p*-value < 0.05 was considered indicative of statistical significance.

3 | RESULTS

3.1 | GF culture and transfection

Primary GFs were extracted from the gingiva of beagles (Figure 2A). The isolated GFs migrated from the tissue within about 10 days. The GFs were typically spindle-shaped with protrusions of various lengths, and the cell bodies were full and showed a typical fibroblastic morphology (Figure 2B). Most lentivirus-transfected cells expressed GFP, indicating successful transfection (Figure 2C).

3.2 | Construction of 3D-bioprinted scaffolds

3D-bioprinted scaffolds with and without GFs were constructed as described previously.³¹ The scaffold had an outer layer with dense pores to increase its strength, and an inner layer with loose pores facilitating the transport of nutrients (Figure 2D,E). The GFs were evenly distributed within the scaffolds under a confocal fluorescent microscope (Figure 2F,G).

3.3 | Animal experiments

We next evaluated the roles of GFs and 3D-bioprinted ADM scaffolds in periodontal keratinized tissue regeneration. All animals in the blank control, ADM cell-free, and ADM cell groups were alive at 2 months after surgery. The preoperative evaluation, surgery, and 2-month postoperative evaluation results are shown in Figure 3.

3.4 | Clinical observations

3.4.1 | Clinical healing

The protective device in the recipient area was removed 2 weeks after surgery, and new reddish tissue was seen in the recipient area. The transplanted 3D-bioprinted scaffold was partially degraded compared with its state immediately post-operation, but residual material remained visible. Two months after surgery, the wounds had completely healed in all three groups. The degree of tissue regeneration differed among the three groups, the tissue was mature, and keratinization was complete. New keratinized tissue in the recipient area was fused with adjacent tissue, and there was no obvious

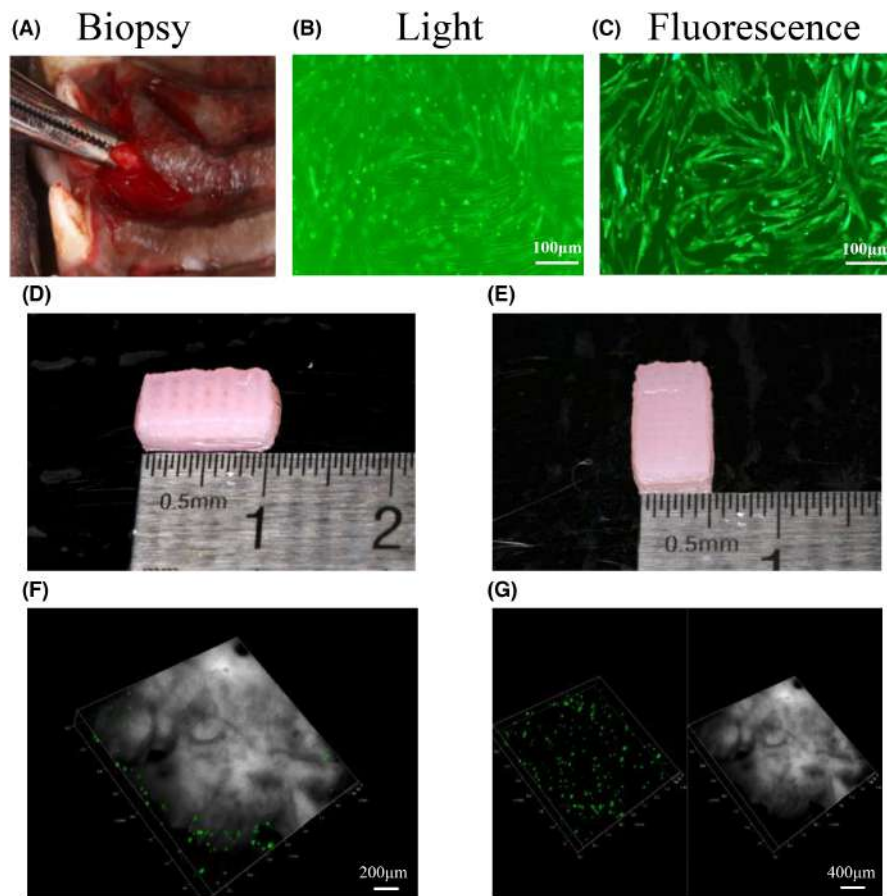


FIGURE 2 Gingival fibroblasts transfection and 3D-bioprinted scaffold construction. (A) Gingiva was collected for GF extraction. (B) Optical and (C) fluorescence micrographs images of GFs transfected with GFP lentivirus. The scaffold was approximately 10 mm long (D) and 5 mm wide (E). (F) The merged image of cells and scaffold under a confocal fluorescent microscope. (G) The separated image of cells and scaffold under a confocal fluorescent microscope. Cells which displayed green fluorescence are widely and uniformly distributed in the scaffold. GFP, green fluorescent protein; GFs, gingival fibroblasts.

scar or fold. All treated sites showed favorable clinical healing with no complications such as swelling, suppuration, or abscess formation (Figure 3).

3.4.2 | Clinical measurements

The widths of keratinized and attached gingiva in ROI at baseline and 2 months thereafter are given in Table S1 (Supplemental Material). The three surgical procedures all increased the keratinized gingiva and attached gingiva after 2-month assessment (Table S1). The keratinized gingiva increased in the buccal mesial, mid, and distal regions in the ADM cell and ADM cell-free groups compared with the blank control group ($p < 0.01$; Figure 4). Also, the increment of keratinized gingiva in the ADM cell group (mesial buccal: 1.93 ± 0.44 mm; mid-buccal: 1.58 ± 0.37 mm; distal buccal: 1.60 ± 0.42 mm) was greater than in the ADM cell-free group (mesial buccal: 0.90 ± 0.29 mm; mid-buccal: 0.67 ± 0.12 mm; distal buccal: 1.30 ± 0.29 mm; $p < 0.01$; Figure 4).

Similarly, more attached gingiva increment was observed in the ADM cell group (mesial buccal: 2.30 ± 0.41 mm; mid-buccal: 1.83 ± 0.33 mm; distal buccal: 1.85 ± 0.44 mm) compared with the ADM cell-free group (mesial buccal: 1.07 ± 0.09 mm; mid-buccal: 0.83 ± 0.12 mm; distal buccal: 1.30 ± 0.29 mm), while in the blank control group (mesial buccal: 0.48 ± 0.04 mm; mid-buccal:

0.38 ± 0.04 mm; distal buccal: 0.45 ± 0.05 mm) the least amount of increment was detected ($p < 0.01$; Figure 4).

3.5 | Histologic analysis

3.5.1 | Descriptive histological outcomes

Green fluorescence was observed in tissue sections of the ADM cell group, but not in the ADM cell-free or blank control group, suggesting that neoplastic tissue formation is related to GFs in the 3D-bioprinted scaffolds (Figure 5).

The degree of periodontal tissue regeneration differed among the three groups. H&E staining showed that tissue healed well in all three groups. No material residue or obvious inflammatory cell infiltration was observed. The structure of the new epithelium was more intact and continuous in the ADM cell group with ADM-free group, while more amorphous construct and non-keratinized epithelium was in the blank control group (Figure 6A–C). Masson staining showed that the density of collagen fibers was greater in the ADM cell and ADM cell-free groups compared with the blank control group. The gingival fibers showed a more orderly arrangement in the ADM cell group compared with the ADM cell-free group (Figure 6D–F). Moreover, Sirius red staining confirmed that more the Type I collagen fiber bundles were arranged in oriented

FIGURE 3 Surgical procedures of the blank control group, ADM cell-free group, and ADM cell group. (A) Baseline status. The KGW of three sites (mesiobuccal, midbuccal, and distobuccal) was measured along the tooth longitudinal axis with reference to the mesial gingiva margin, midpoint of gingiva margin (corresponding to the midpoint of the tooth cusp), and distal gingiva margin of the tooth. (B) A 1.5-cm-long horizontal incision was made along the mucogingival junction. (C) A partial-thickness flap was turned toward the root and repositioned apically. (D) No implant was placed in the blank control group. ADM cell-free and ADM cell scaffolds were placed in the ADM cell-free and ADM cell groups, respectively. (E) Placement of aluminum foil for protection after suturing. (F) 2 months after surgery. The measurements were performed as the baseline. KGW, width of keratinized gingiva.

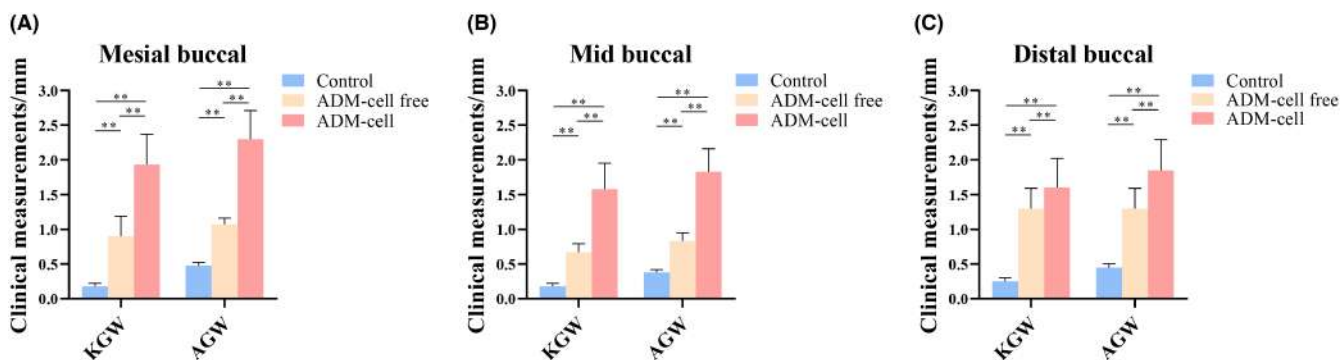
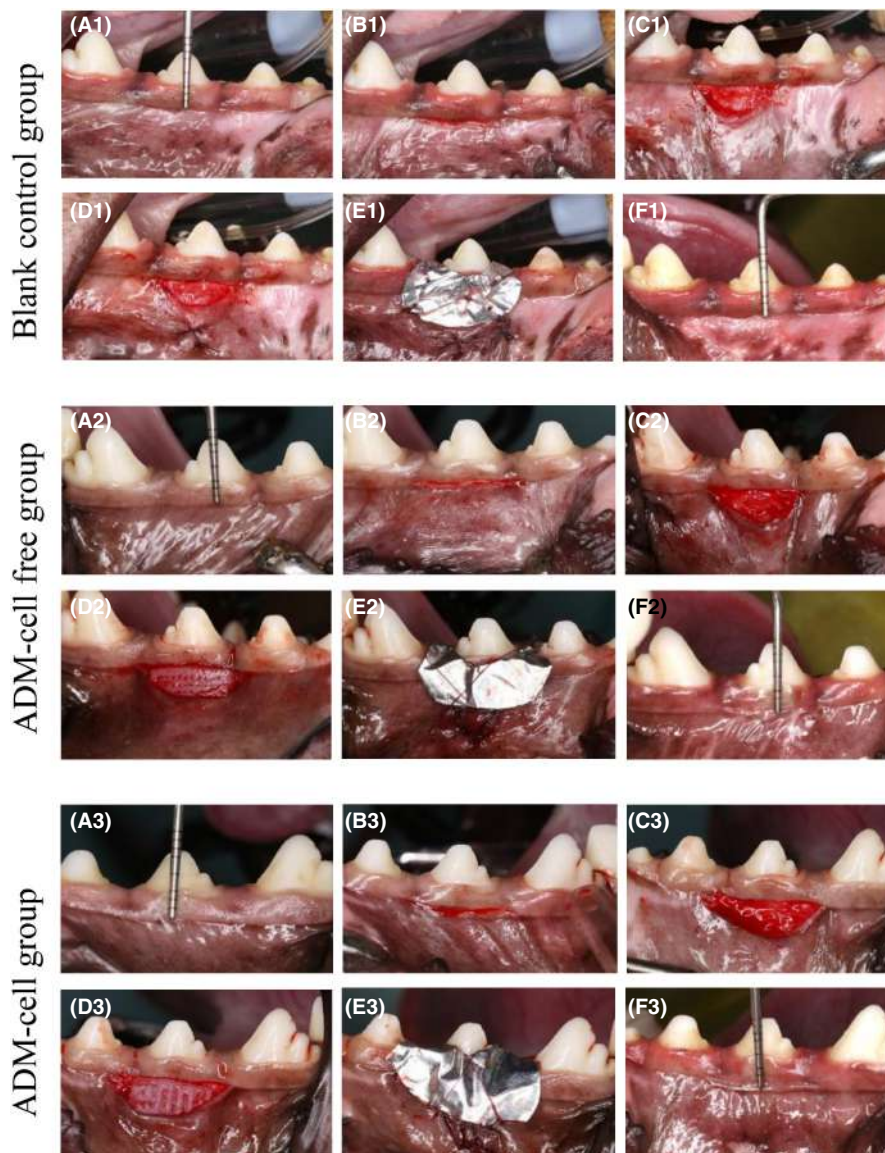


FIGURE 4 The width augmentation of keratinized gingiva and attached gingiva in mesiobuccal (A), midbuccal (B), and distal buccal (C) in the blank control group, ADM cell-free group, and ADM cell group. The width of the attached gingiva (AGW) is the difference between the KGW and PD. KGW is the width of keratinized gingiva; PD, probing depth; AGW: the width of attached gingiva. (** $p < 0.01$).

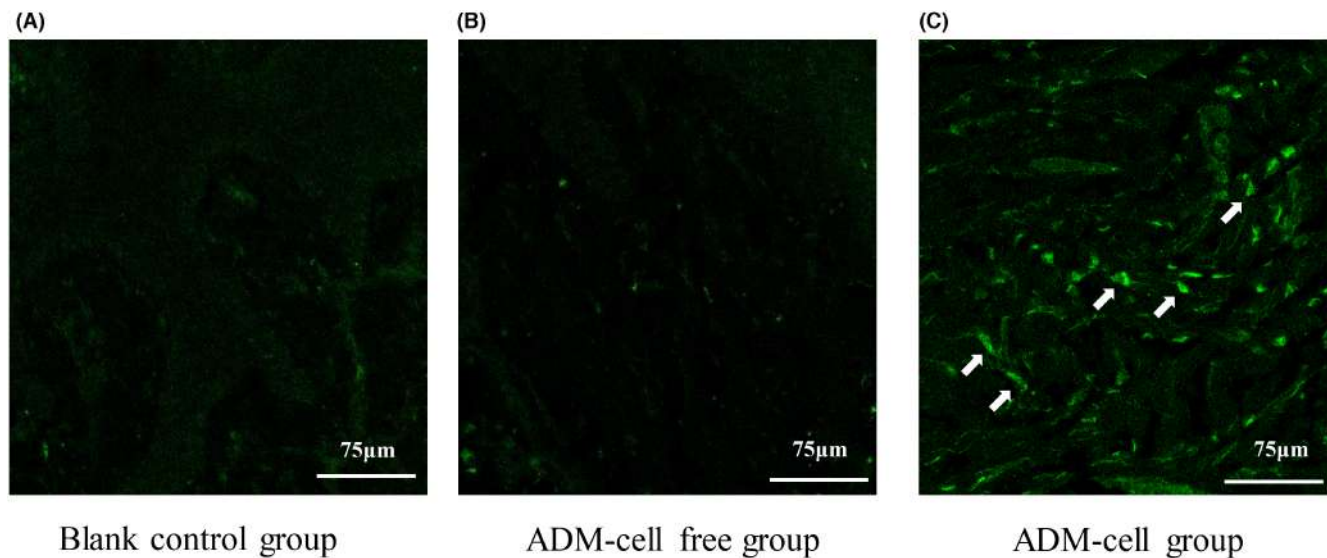


FIGURE 5 Confocal laser micrograph of a tissue section. (A) Blank control group. (B) ADM cell-free group. (C) ADM cell group. Arrows indicate GFP-labeled cells expressing green fluorescence.

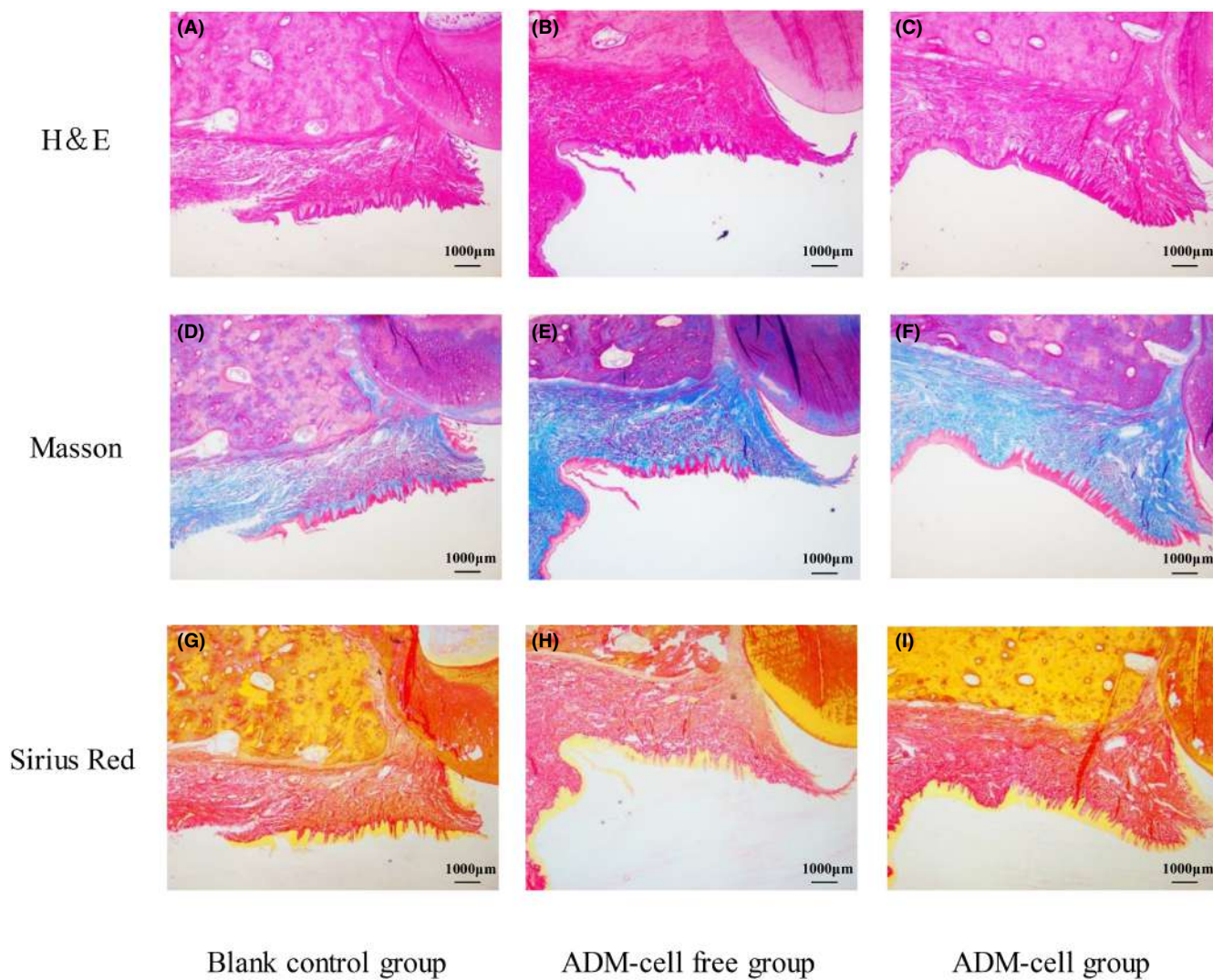


FIGURE 6 H&E (A–C), Masson (D–F), and Sirius red (G–I) staining of gingiva in the blank control, ADM cell-free, and ADM cell groups.

order in the ADM cell group compared with the ADM cell-free group (Figure 6G-I).

3.5.2 | COL I, COL III, and VEGF-A expression

VEGF mainly targeting endothelial cells, plays an important role in vasculogenesis and angiogenesis.³² VEGF-A immunostaining was observed in three groups. We found that VEGF-A expression was significantly higher in the ADM cell-free and ADM cell groups than that in the blank control group. And the expression was higher in the ADM cell group than that in the ADM cell-free group (Figure 7A-C,J). VEGF-A Expression was strongly positive around the blood vessels.³² More blood vessels were observed in the ADM cell group compared with the ADM cell-free group, while in the blank control group, the least amount of blood vessels was detected (Figure 7A-C). COL I and COL III are principal components in the gingival extracellular matrix.³³ COL I expression was the highest in the ADM cell group, followed by the ADM cell-free group and the blank control group (Figure 7D-F,K). Similarly, COL III expression was the highest in the ADM cell group, followed by the ADM cell-free group, and the lowest in the blank control group (Figure 7G-I,L). These results indicated that ADM scaffolds and GFs may be helpful in the process of new blood vessels and collagen formation in gingival tissue regeneration.

4 | DISCUSSION

The field of tissue engineering has progressed tremendously over the past few decades in terms of its ability to fabricate functional tissue substitutes.³⁴⁻³⁶ 3D-bioprinting can mimic the complex microstructures of biological tissues. Periodontal tissue regeneration using ADM is performed because of its good biocompatibility and esthetics.^{37,38} Using 3D-bioprinting technology to deposit ADM materials with micrometer precision in cell-friendly conditions will facilitate keratinized gingival regeneration.

ADM has good biocompatibility and can be used to treat gingival recession.³⁹ Moreover, ADM can be used as a graft material to replace autologous connective tissue, increasing the amount of soft tissue and covering the root surface.⁴⁰ In this study, implantation of ADM scaffolds into the beagle oral cavity significantly increased the width of the keratinized gingiva/attached gingiva in the surgical area (0.67–1.30 mm/0.83–1.30 mm versus 0.18–0.25 mm/0.38–0.48 mm). Therefore, ADM scaffolds can promote the regeneration of periodontal keratinized tissue, consistent with previous reports.^{41,42}

In our previous study, the 3D-bioprinted gingival fibroblast-encapsulated scaffold has proved good biological characteristics *in vitro*.³¹ In this study, the final keratinized gingiva increment in the ADM cell group was 1.58–1.93 mm, and the attached gingiva

increment was 1.83–2.30 mm, compared with 0.67–1.30 and 0.83–1.30 mm, respectively, in the ADM cell-free group. The significant difference in tissue increment between the two groups suggests that the 3D-bioprinted GF-encapsulated scaffold had a greater promotive effect on soft tissue regeneration than the simple scaffold. We used GFs because they have homology with gingival tissue and their secreted growth factors promote tissue repair.⁴³ *In vitro* expansion of GFs provides a potential therapeutic strategy for personalized repair of soft tissue defects.

Seed cells play an important role in tissue engineering to promote soft tissue regeneration.⁴⁴⁻⁴⁶ However, some studies have shown that there is no significant difference in the augmentation of keratinized gingiva between cell-containing and cell-free scaffolds. Lotfi et al. implanted scaffolds with and without GFs into the beagle oral cavity; there was no significant difference in the curative effect.²⁸ The increase in the amount of keratinized gingiva was significantly greater in the cell-containing than the scaffold group, possibly because of the use of 3D-bioprinting. Unlike traditional tissue engineering, 3D-bioprinted scaffolds, which have interconnected pores and a large surface area, support cell attachment, growth, communication, and exchange of gas and nutrients. They also enable the precise placement of cells and biomaterials layer-by-layer, thereby mimicking the microstructures of tissue. Loading of cells on the scaffold surface or simply mixing them hampers their function, possibly explaining the different effects of scaffolds without and with cells.

The wound had completely healed 2 months after surgery, and no scar or abnormal color was found. This healing effect is mainly attributed to the properties of the cells and biomaterials, and their promotion of tissue healing.⁴⁷ Histologically, there was no inflammatory infiltration in the healed tissue, and the material was completely absorbed. New tissue encompassed dense connective tissue supporting a keratinized epithelium, consistent with the histological appearance of new keratinized gingiva in previous studies.^{44,46}

This study has several limitations. The number of animals was small, which may have affected the statistical analysis. In addition, the absence of histological assessments at multiple time points during the early stages of healing precludes further assessment of tissue healing and the possibility of providing guidance for protocols aiming to promote tissue gain. Besides, long-term observation is required to evaluate stability and long-term efficacy.

5 | CONCLUSION

In conclusion, the 3D-bioprinted GF-encapsulated ADM scaffolds increased the amount of keratinized gingiva *in vivo*, suggesting that they have great potential for keratinized gingival augmentation. These findings offer a potential therapeutic strategy for periodontal tissue defects and provide new insight into soft tissue regeneration.

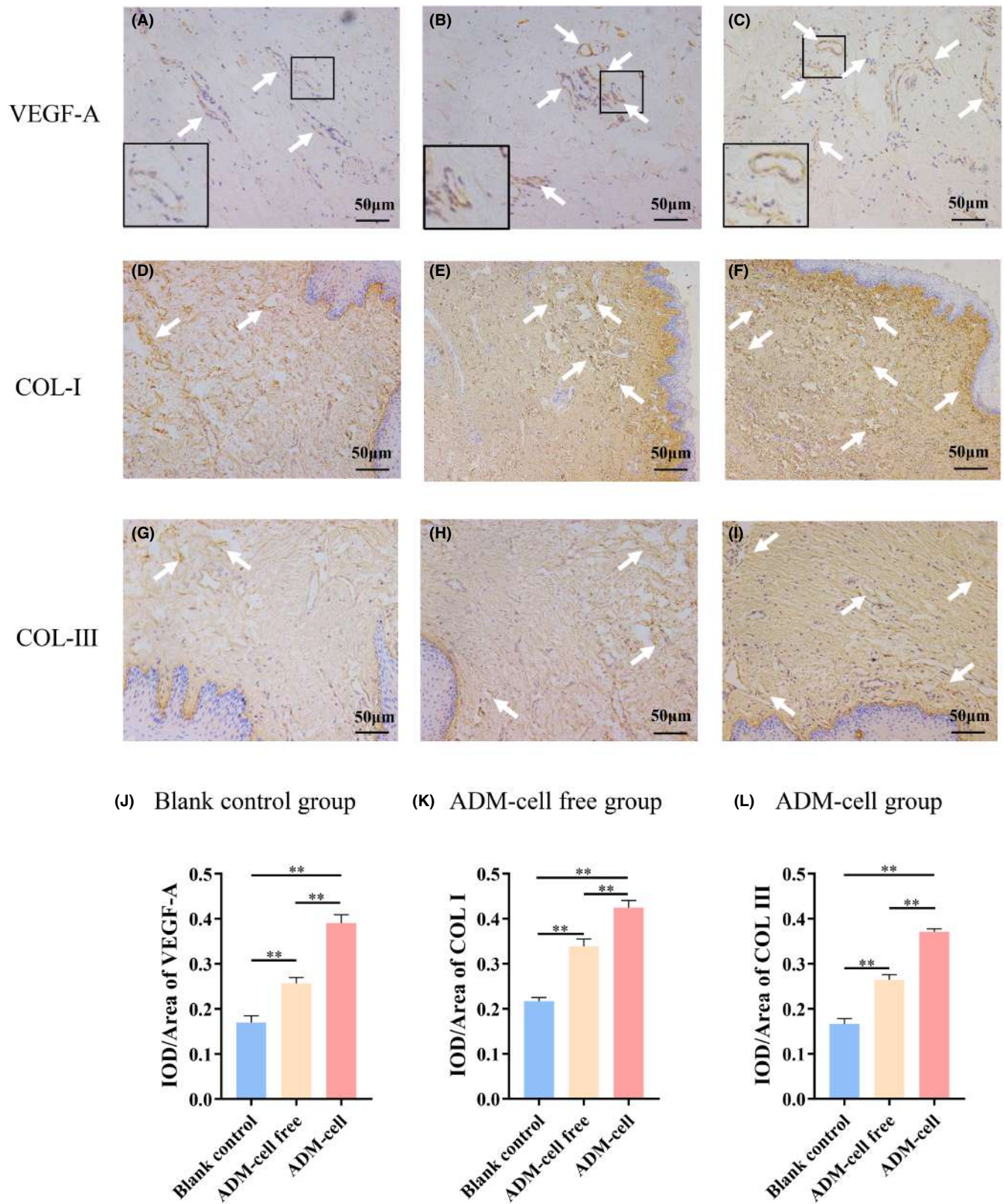


FIGURE 7 Immunohistochemical staining for VEGF-A (A-C), COL I (D-F), and COL III (G-I) in the blank control group, ADM cell-free group, and ADM cell group. The arrows indicate VEGF-A-positive cells (A-C), COL I (D-F), and COL III (G-I). Histogram (J-L) showed the quantification of the immunohistochemical staining. (** $p < 0.01$).

ACKNOWLEDGEMENTS

This study was supported by the National Key Research and Development Program of China (2017YFA0701302), and the Foundation PKUSS20200113.

FUNDING INFORMATION

National Key Research and Development Program of China (2017YFA0701302); Foundation PKUSS20200113.

CONFLICT OF INTEREST STATEMENT

The authors declare no competing interests.

DATA AVAILABILITY STATEMENT

The data that support the findings of this study are available from the corresponding author upon reasonable request.

REFERENCES

- Lang NP, Loe H. The relationship between the width of keratinized gingiva and gingival health. *J Periodontol.* 1972;43:623-627.
- Stetler KJ, Bissada NF. Significance of the width of keratinized gingiva on the periodontal status of teeth with submarginal restorations. *J Periodontol.* 1987;58:696-700.
- Gobbato L, Avila-Ortiz G, Sohrabi K, Wang CW, Karimbux N. The effect of keratinized mucosa width on peri-implant health: a systematic review. *Int J Oral Maxillofac Implants.* 2013;28:1536-1545.
- Lin GH, Chan HL, Wang HL. The significance of keratinized mucosa on implant health: a systematic review. *J Periodontol.* 2013;84:1755-1767.
- Chambrone L, Tatakis DN. Periodontal soft tissue root coverage procedures: a systematic review from the AAP regeneration workshop. *J Periodontol.* 2015;86:S8-S51.
- Brasher WJ, Rees TD, Boyce WA. Complications of free grafts of masticatory mucosa. *J Periodontol.* 1975;46:133-138.
- Pack AR, Gaudie WM, Jennings AM. Bony exostosis as a sequelae to free gingival grafting: two case reports. *J Periodontol.* 1991;62:269-271.
- Bertl K, Melchard M, Pandis N, Muller-Kern M, Stavropoulos A. Soft tissue substitutes in non-root coverage procedures: a systematic review and meta-analysis. *Clin Oral Investig.* 2017;21:505-518.
- Shridharani SM, Tufaro AP. A systematic review of acellular dermal matrices in head and neck reconstruction. *Plast Reconstr Surg.* 2012;130:355-435.
- Zheng M, Wang X, Chen Y, et al. A review of recent progress on collagen-based biomaterials. *Adv Healthc Mater.* 2022:e2202042. Online ahead of print.
- Scarano A, Barros RR, Iezzi G, Piattelli A, Novaes AB Jr. Acellular dermal matrix graft for gingival augmentation: a preliminary clinical, histologic, and ultrastructural evaluation. *J Periodontol.* 2009;80:253-259.
- Guo J, Chen H, Wang Y, Cao CB, Guan GQ. A novel porcine acellular dermal matrix scaffold used in periodontal regeneration. *Int J Oral Sci.* 2013;5:37-43.
- Moraschini V, Guimaraes HB, Cavalcante IC, Calasans-Maia MD. Clinical efficacy of xenogeneic collagen matrix in augmenting keratinized mucosa round dental implants: a systematic review and meta-analysis. *Clin Oral Investig.* 2020;24:2163-2174.
- Tavelli L, Barootchi S, Di Gianfilippo R, et al. Acellular dermal matrix and coronally advanced flap or tunnel technique in the treatment of multiple adjacent gingival recessions. A 12-year follow-up from a randomized clinical trial. *J Clin Periodontol.* 2019;46:937-948.
- Liu P, Li Q, Yang Q, Tang Z. Three-dimensional cell printing of gingival fibroblast/acellular dermal matrix/gelatin-sodium alginate scaffolds and their biocompatibility evaluation in vitro. *RSC Adv.* 2020;10:10.
- Mironov V, Reis N, Derby B. Review: bioprinting: a beginning. *Tissue Eng.* 2006;12:631-634.
- Wlodarczyk-Biegun MK, Del Campo A. 3D bioprinting of structural proteins. *Biomaterials.* 2017;134:180-201.
- Matai I, Kaur G, Seyedsalehi A, McClinton A, Laurencin CT. Progress in 3D bioprinting technology for tissue/organ regenerative engineering. *Biomaterials.* 2020;226:119536.
- Zhou X, Nowicki M, Sun H, et al. 3D bioprinting-tunable small-diameter blood vessels with biomimetic biphasic cell layers. *ACS Appl Mater Interfaces.* 2020;12:45904-45915.
- Baltazar T, Merola J, Catarino C, et al. Three dimensional bioprinting of a vascularized and perfusable skin graft using human keratinocytes, fibroblasts, pericytes, and endothelial cells. *Tissue Eng Part A.* 2020;26:227-238.
- Murphy SV, De Coppi P, Atala A. Opportunities and challenges of translational 3D bioprinting. *Nat Biomed Eng.* 2020;4:370-380.
- Ying Li HY, Chen W, et al. Peripheral nerve regeneration with 3D printed bionic scaffolds loading neural crest stem cell derived Schwann cell progenitors. *Adv Funct Mater.* 2021;2010215:1-16.
- Zhang J, Wehrle E, Rubert M, Muller R. 3D bioprinting of human tissues: biofabrication, bioinks, and bioreactors. *Int J Mol Sci.* 2021;22:3971-3991.
- Hong N, Yang GH, Lee J, Kim G. 3D bioprinting and its in vivo applications. *J Biomed Mater Res B Appl Biomater.* 2018;106:444-459.
- Vijayavenkataraman S, Yan WC, Lu WF, Wang CH, Fuh JYH. 3D bioprinting of tissues and organs for regenerative medicine. *Adv Drug Deliv Rev.* 2018;132:296-332.
- Moncal KK, Gudapati H, Godzik KP, et al. Intra-operative bioprinting of hard, soft, and hard/soft composite tissues for craniomaxillofacial reconstruction. *Adv Funct Mater.* 2021;31:2010858.
- Fassake TMK. Comparative stomatoscopic and histochemical studies of the marginal gingiva in man. *Parodontol.* 1958;12:151-160.
- Lotfi G, Shokrgozar MA, Mofid R, et al. A clinical and histologic evaluation of gingival fibroblasts seeding on a chitosan-based scaffold and its effect on the width of keratinized gingiva in dogs. *J Periodontol.* 2011;82:1367-1375.
- Somerman MJ, Archer SY, Imm GR, Foster RA. A comparative study of human periodontal ligament cells and gingival fibroblasts in vitro. *J Dent Res.* 1988;67:66-70.
- Tanaka K, Iwasaki K, Feghali KE, Komaki M, Ishikawa I, Izumi Y. Comparison of characteristics of periodontal ligament cells obtained from outgrowth and enzyme-digested culture methods. *Arch Oral Biol.* 2011;56:380-388.
- Liu P, Li Q, Yang Q, et al. Three-dimensional cell printing of gingival fibroblast/acellular dermal matrix/gelatin-sodium alginate scaffolds and their biocompatibility evaluation in vitro. *RSC Adv.* 2020;10:15926-15935.
- Apte RS, Chen DS, Ferrara N. VEGF in signaling and disease: beyond discovery and development. *Cell.* 2019;176:1248-1264.
- Liao W, Okada M, Sakamoto F, et al. In vitro human periodontal ligament-like tissue formation with porous poly-L-lactide matrix. *Mater Sci Eng C Mater Biol Appl.* 2013;33:3273-3280.
- Wang Z, Wang L, Li T, et al. 3D bioprinting in cardiac tissue engineering. *Theranostics.* 2021;11:7948-7969.
- Tang M, Rich JN, Chen S. Biomaterials and 3D bioprinting strategies to model glioblastoma and the blood-brain barrier. *Adv Mater.* 2021;33:e2004776.
- Cadena M, Ning L, King A, et al. 3D bioprinting of neural tissues. *Adv Healthc Mater.* 2021;10:e2001600.
- Gallagher SI, Matthews DC. Acellular dermal matrix and subepithelial connective tissue grafts for root coverage: a systematic review. *J Indian Soc Periodontol.* 2017;21:439-448.

38. Shanmugam M, Sivakumar V, Anitha V, Sivakumar B. Clinical evaluation of alloderm for root coverage and colour match. *J Indian Soc Periodontol*. 2012;16:218-223.
39. Amine K, El Amrani Y, Chemlali S, Kissa J. Alternatives to connective tissue graft in the treatment of localized gingival recessions: a systematic review. *J Stomatol Oral Maxillofac Surg*. 2018;119:25-32.
40. Kroiss S, Rathe F, Sader R, Weigl P, Schlee M. Acellular dermal matrix allograft versus autogenous connective tissue grafts for thickening soft tissue and covering multiple gingival recessions: a 5-year preference clinical study. *Quintessence Int*. 2019;50:278-285.
41. Chambrone L, Ortega MAS, Sukekava F, et al. Root coverage procedures for treating single and multiple recession-type defects: an updated Cochrane systematic review. *J Periodontol*. 2019;90:1399-1422.
42. Cortellini P, Bissada NF. Mucogingival conditions in the natural dentition: narrative review, case definitions, and diagnostic considerations. *J Periodontol*. 2018;89(Suppl 1):S204-S213.
43. Rodrigues AZ, Oliveira PT, Novaes AB Jr, Maia LP, Souza SL, Palioto DB. Evaluation of in vitro human gingival fibroblast seeding on acellular dermal matrix. *Braz Dent J*. 2010;21:179-189.
44. Prato GP, Rotundo R, Magnani C, Soranzo C, Muzzi L, Cairo F. An autologous cell hyaluronic acid graft technique for gingival augmentation: a case series. *J Periodontol*. 2003;74:262-267.
45. McGuire MK, Nunn ME. Evaluation of the safety and efficacy of periodontal applications of a living tissue-engineered human fibroblast-derived dermal substitute. I. Comparison to the gingival autograft: a randomized controlled pilot study. *J Periodontol*. 2005;76:867-880.
46. Mohammadi M, Shokrgozar MA, Mofid R. Culture of human gingival fibroblasts on a biodegradable scaffold and evaluation of its effect on attached gingiva: a randomized, controlled pilot study. *J Periodontol*. 2007;78:1897-1903.
47. Novaes AB Jr, Marchesan JT, Macedo GO, Palioto DB. Effect of in vitro gingival fibroblast seeding on the in vivo incorporation of acellular dermal matrix allografts in dogs. *J Periodontol*. 2007;78:296-303.

SUPPORTING INFORMATION

Additional supporting information can be found online in the Supporting Information section at the end of this article.

How to cite this article: Liu P, Li Q, Yang Q, et al. Evaluation of the effect of 3D-bioprinted gingival fibroblast-encapsulated ADM scaffolds on keratinized gingival augmentation. *J Periodont Res*. 2023;58:564-574. doi:[10.1111/jre.13126](https://doi.org/10.1111/jre.13126)